Stability of lutetium microclusters: Molecular-dynamics simulations

T. Baştuğ, Ş. Erkoç,* M. Hirata, and S. Tachimori
Department of Materials Science, JAERI, Tokai-mura, Naka-gun, Ibaraki 319-11, Japan
(Received 18 September 1998)

Structural stability and energetics of lutetium microclusters $Lu_n(n=3-147)$ have been investigated by molecular-dynamics simulations. An empirical model potential energy function has been parametrized for the lutetium element by using the dimer interaction potential energy profile of Lu_2, which is calculated by the relativistic density functional method. Stable structures of the microclusters for $n=3-13$ have been determined by a molecular-dynamics simulation. It has been found that lutetium microclusters prefer to form three-dimensional compact structures. Molecular-dynamics simulations have also been performed for spherical lutetium clusters generated from hcp crystal structure with sizes $n=33-147$. [S1050-2947(99)08405-X]

PACS number(s): 36.40.Cg, 31.15.Qg

I. INTRODUCTION

Clusters play an important role in understanding the transition from the microscopic structure to the macroscopic structure of matter. The research field of clusters, particularly microclusters, has shown rapid development in both experimental and theoretical investigations in the last two decades [1–3]. Although there has been considerable improvement in the experimental techniques, there are still difficulties in the production and/or investigation of isolated microclusters of some elements. Computer simulations provide help for a deeper understanding of the experimental observations on the one hand, and they can also be applied for systems which are practically difficult to experiment on, on the other hand. Atomistic level computer simulations using empirical model potentials have been used successfully to investigate bulk, surface, and cluster properties of elements. Several empirical potential energy functions have been proposed and applied to various systems in the last decade [4].

Lutetium microclusters are interesting and have potential importance in the physics and chemistry of lantanides [5]. Although there is theoretical and experimental information about the molecules and/or clusters containing lutetium atoms in the literature [6], this information is limited for systems containing only one lutetium atom. Only the binding energy of the lutetium dimer is available as experimental information [7]. Although the large-scale *ab initio* computations are possible these days, the electronic and geometric structures of lutetium microclusters have not been studied yet.

In this work we will investigate the structural properties of isolated lutetium microclusters containing 3 to 147 atoms using a pair potential as a first approximation. First we perform the total energy calculations for the lutetium dimer by using relativistic density functional theory (RDFT). The potential energy profile of the lutetium dimer will be obtained. Although density functional methods have been used in many-atom systems [8], it is still difficult with the available computer facilities to optimize the geometry of many-atom systems containing heavy elements. Therefore we will parametrize an empirical potential energy function (PEF) for the Lutetium element. Using the empirical PEF we performed molecular–dynamics (MD) simulations to predict the optimum geometries of lutetium microclusters.

II. RDFT CALCULATION FOR DIMER

Relativistic effects remarkably influence the electronic structure and the chemical bonding of heavy atoms [9,10]. The main effects, such as the spin-orbit interaction, mass-velocity, and Darvin terms lead to a substructure and contraction of electronic shells. These affect the electronic structure, and thus the chemical bonding. In order to fully include all relativistic effects a four-component relativistic formulation is essential [11].

In this work, we first calculated the geometric structure of the Lu-dimer with an *ab initio* all-electron fully relativistic density functional method [12]. The total energy is expressed as a functional of charge density $\rho(r)$,

$$E[\rho]=\sum_i n_i\langle\phi_i|t|\phi_i\rangle-\int \rho V^n + \tfrac{1}{2}\int \rho V^c-E^{xc}+\sum_{p>q}\frac{Z_pZ_q}{|R_p-R_q|}, \qquad (2.1)$$

where t is the Dirac kinetic energy operator, a 4×4 matrix in spinor space, V^n represents the potential energy of the interaction of the electrons with the nuclei, and V^c is the direct Coulomb-interaction potential among the electrons. The last two terms represent the exchange-correlation and the nucleus-nucleus Coulomb interaction energies, respectively. The total energy functional $E[\rho]$, Eq. (2.1), has a minimum with the ground state density ρ of the system. Application of the variational principle with the constraint of conservation of the number of electrons leads to the single particle Kohn-Sham equations

$$[t+V^n+V^c+V^{xc}]|\phi_i\rangle=\varepsilon_i|\phi_i\rangle. \qquad (2.2)$$

*Present address: Department of Physics, Middle East Technical University, 06531 Ankara, Turkey.

The exchange-correlation potential V^{xc} is a functional derivative of the exchange-correlation energy E^{xc} with respect to the density, that is,

$$\rho(r)=\sum_i n_i \phi_i^{\dagger}(r)\phi_i(r), \tag{2.3}$$

where n_i are the occupation numbers. The parametrized exchange-correlation potential of Vosko, Wilke, Nusair [13] is used for the local density approximation. The generalized gradient approximation (GGA) of Becke [14] is included perturbatively in order to consider nonlocal contributions. In both LDA and GGA level calculations, the relativistic form of the exchange-correlation potentials, which was developed by Engel *et al.* [15], has been used.

In order to solve the Kohn-Sham equations we used the molecular-orbital–linear-combination-of-atomic-orbitals (MO-LCAO) approach. The molecular wave functions ϕ_i are expanded into the symmetry adapted orbitals χ_j, which are also expanded in terms of the atomic orbitals $\xi_{n_\nu}(r)$. These atomic orbitals are four-component Dirac spinors. The symmetrization coefficients are obtained by the use of group theoretical projection operators [16]

$$\phi_i(r)=\sum_j \chi_j c_{ji}=\sum_j \xi_{n_\upsilon}(r) d_{n_\upsilon j} c_{ji}, \tag{2.4}$$

where $n_\upsilon=(\nu,n,\kappa,m)$. Here υ indicates atomic site and m and κ are magnetic and Dirac quantum numbers. The variational coefficients are determined by using standard procedure for solving the secular equation

$$\mathbf{HC}=\varepsilon\mathbf{SC}, \tag{2.5}$$

where **H** and **S** are the Hamiltonian and overlap matrices, respectively. The matrix elements are evaluated numerically by using the modified version for relativistic numerical wave functions [17] of the integration scheme of Boerrigter, Velde, and Baerends [18]. The direct Coulomb potential V^c has been calculated via an additional variational procedure, which reduces the numerical errors and yields a variationally consistent total energy [11].

The numerical $(1s\text{-}6p)$ Kohn-Sham orbitals of the Lu atom are chosen as the basis set. The binding energy of the Lu_2 is calculated as a difference of total energies of the Lu_2 molecule and Lu atoms in their ground states. The atomic total energies are calculated by the molecule code in order to increase the numerical accuracy.

The calculated potential energy curve of the Lu_2 molecule has been presented in Fig. 1 together with the fitted PEF. We have estimated the spectroscopic constants of the Lu dimer as $r_e=2.510$ Å, $D_e=2.388$ eV, and $\omega_e=174$ cm^{-1}. Comparing to the experimental binding energy [7] of 1.47 eV, our estimation is relatively deep. It is well known that density functional methods give over estimated binding energies, but good bond distances. To our knowledge there is no experimental bond distance and vibration frequency available in the literature for Lu_2.

In order to study the role of the partially filled *d*-like and unoccupied *p*-like KS atomic orbitals in the bonding, we applied the Mulliken's population analysis for Lu-dimer calculations. The main contribution to the bond formation of the Lu-dimer are due to the $5d\text{-}5d$, $6s\text{-}6s$, and $6p\text{-}5d$ overlaps. The bond overlap populations are 0.334 for $5d\text{-}5d$, 0.274 for $6s\text{-}6s$, and 0.234 for $6p\text{-}5d$. The $6s\text{-}6p$, $6p\text{-}6p$, and $6s\text{-}5d$ overlaps are relatively small compared with the $5d\text{-}5d$ interaction. The $4f$ orbitals are located energetically deeper, so that the contribution of the $4f$ orbitals to the bond formation is negligible. The Mulliken's population analysis shows the importance of the *d*- and *p*-like KS orbitals in the bonding. A potential energy calculation with a basis set excluding unoccupied *p* orbitals gives a bond distance of $r_e=2.550$ Å and a binding energy of $D_e=1.45$ eV. Although this value agrees better with experimental result of binding energy, the basis set is less complete compared to the basis set including *p* orbitals.

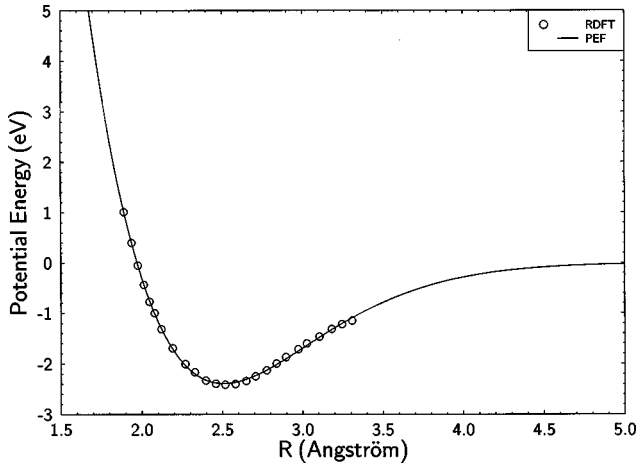

FIG. 1. Potential energy curve of Lu_2. Circles represent the RDFT results, and the full line represents the fitted empirical pair-potential energy function.

III. PARAMETRIZATION OF THE PEF

We have expressed the pair potential energy function of the dimer as the recently developed empirical function, which works well for transition metals [19]. The empirical pair potential energy function $U(r)$ is in the form

$$U(r)=\frac{A_1}{r^{\lambda_1}}e^{-\alpha_1 r^2}+\frac{A_2}{r^{\lambda_2}}e^{-\alpha_2 r^2}. \tag{3.1}$$

The first term represents the repulsive branch and the second term represents the attractive branch of the interaction potential between two atoms. By performing a nonlinear least square fit procedure the parameters $(A_1,\alpha_1,\lambda_1;A_2,\alpha_2,\lambda_2)$ of the empirical pair potential are determined. In the fit procedure we have used the binding energy values of Lu_2 calculated at various interatomic distances by RDFT. The estimated points by RDFT and the fitted function are shown in Fig. 1. The potential parameters for lutetium are determined as $A_1=165.954552$, $A_2=-90.3411822$, $\lambda_1=0.681183981$, $\lambda_2=0.911960557$, $\alpha_1=0.470134794$, $\alpha_2=0.273350677$. In these parameters energy is in eV, and distance is in Å.

The total interaction energy (Φ) of an N particle system may be calculated from the sum of pair interactions

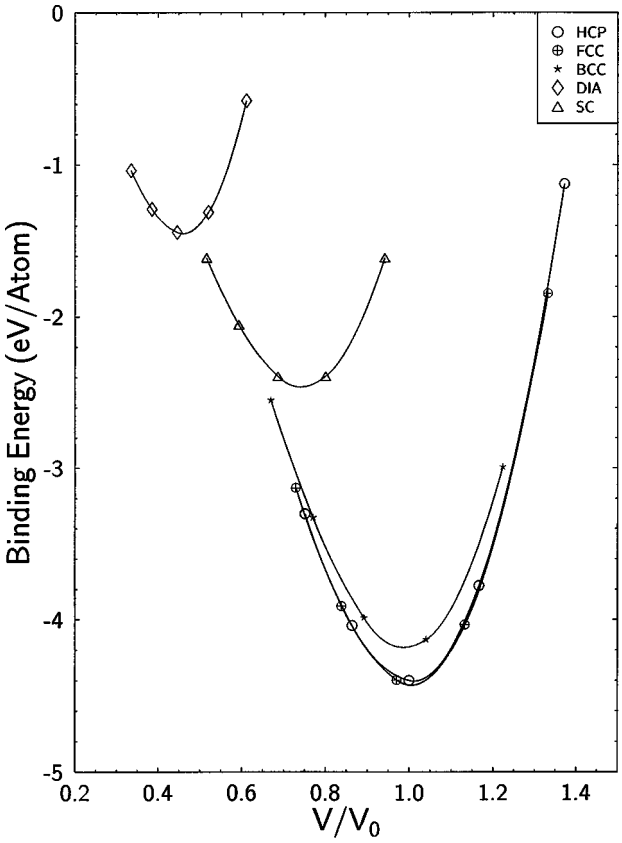

FIG. 2. Variation of cohesive energy with respect to atomic volume for various crystal structures.

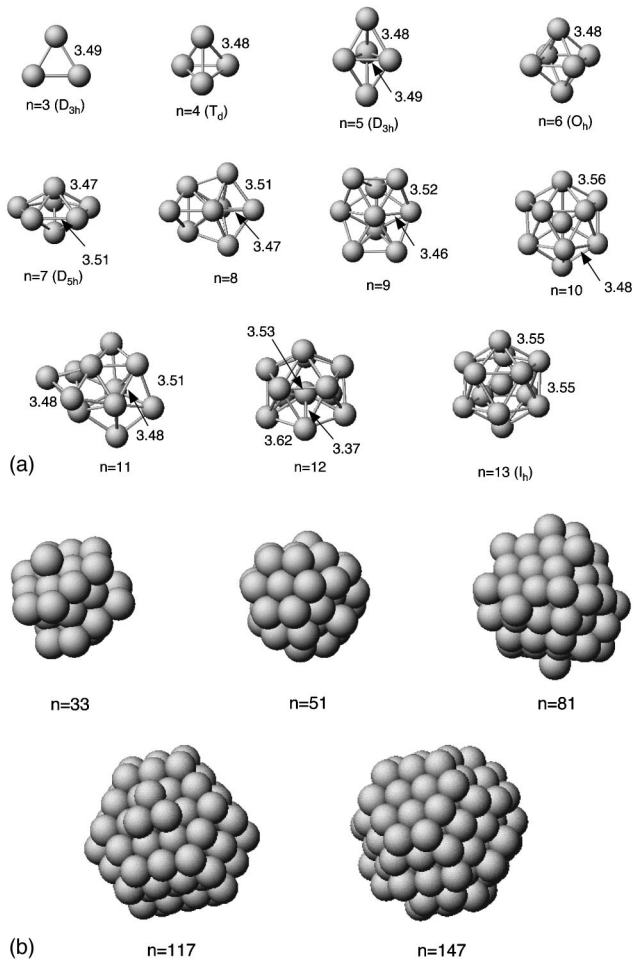

FIG. 3. (a) Equilibrium structures of lutetium microclusters for $n=3-13$, (b) equilibrated spherical clusters generated from the hcp structure.

$$\Phi=\sum_{i<j}^{N} U(r_{ij}). \tag{3.2}$$

Due to the lack of many-body interactions in the potential energy function, the calculated cohesive energy by using Eq. (3.2) might be too much lower than the experimental value. In order to overcome this deficiency one may scale the total interaction energy to the experimental bulk value by separating the pair energy into two parts as repulsive $U_{21}(r)$ and attractive $U_{22}(r)$ terms [19]. The final form of the potential energy function containing the many-body contributions may then be expressed as

$$\Phi=D_{21}\sum_{i<j}^{N} U_{21}(r_{ij})+D_{22}\sum_{i<j}^{N} U_{22}(r_{ij}). \tag{3.3}$$

The additional parameters (D_{21},D_{22}) may be determined analytically from the total interaction energy expression, Eq. (3.3), and the bulk stability condition $\partial\Phi/\partial V=0$ at $T=0$ K. The combination $D_{21}U_{21}(r)+D_{22}U_{22}(r)$ represents the effective pair interaction [19]. The lattice sums have been calculated using the hcp crystal structure for lutetium with the lattice constants $a=3.50$ and $c=5.55$ Å [20]. We have used the value of -4.40 eV for bulk cohesive energy [21]. A nine digit accuracy is obtained in the lattice sums. The additional parameters calculated for the lutetium PEF are $D_{21}=2.51086634$, $D_{22}=0.902502748$, which are unitless numbers. Therefore, the present empirical potential energy function for the lutetium element satisfies the dimer potential, the bulk cohesive energy, and the bulk stability condition exactly. The present PEF also satisfies the crystal stability. The variation of cohesive energy with respect to the atomic volume for various crystal structures are shown in Fig. 2, hcp and fcc structures have almost the same energy versus volume profile. Using this PEF we performed molecular-dynamics simulations to obtain the most stable structures of lutetium microclusters with the number of atoms from 3 to 147. A similar PEF with different parameter sets was successful to simulate bulk and cluster properties of Cu, Ag, and Au elements [19], and nanowire properties of Cu [22]. We expect that we may also use this PEF for the cluster properties of lutetium.

IV. RESULTS AND DISCUSSION

Lutetium microclusters having 3 to 147 atoms have been investigated by performing a molecular-dynamics simulation at constant temperature to obtain the most stable structure of

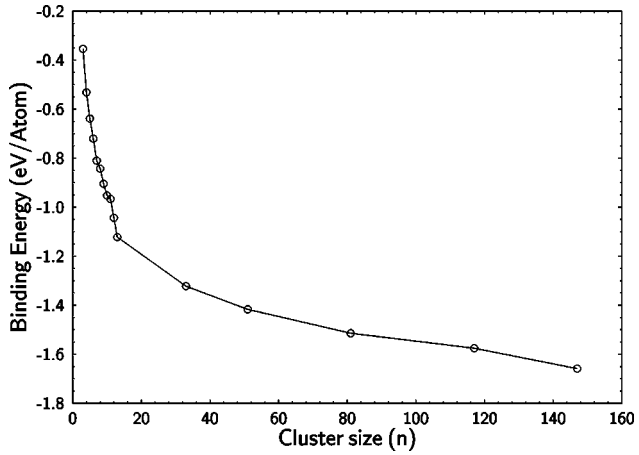

FIG. 4. Average interaction energy per atom (binding energy E_b) versus cluster size (n).

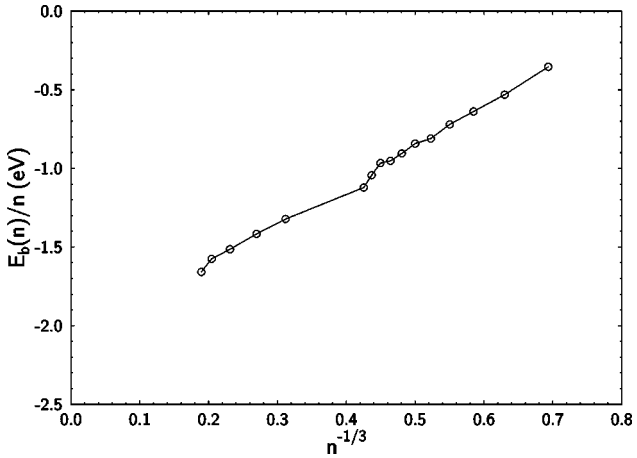

FIG. 5. Average interaction energy per atom (binding energy E_b) versus cluster size ($n^{-1/3}$).

each cluster. In the MD simulations the parametrized empirical PEF was used. The simulations were carried out by starting at 600 K, then the temperature is reduced to 1 K. We have done this procedure in order to increase the probability of catching the global minimum of the potential energy surface of the simulated cluster. The time step has been taken as 2.2×10^{-15} sec. In the simulations we have taken 90 000 as the maximum number of MD steps. This number of steps was enough to reach the equilibrium in total energy and to get the thermal equilibrium of the system studied.

As with conventional molecules, most clusters, in general, have a well-defined geometry corresponding to the absolute minimum energy of their potential surfaces. There might be many local minima on the potential energy surface of a many-particle system. In the present study we generated the microclusters starting from three particles. After obtaining the most stable structure by the quenching procedure we added one atom to obtain the next cluster, and repeated the quenching procedure. We applied this method for the microclusters with sizes $n=3-13$. For each cluster model we obtained a unique structure, without any isomer. The most stable structures of lutetium microclusters with sizes $n=3-13$ obtained by the MD simulations are shown in Fig. 3(a). These structures represent the configuration of the system studied at the last MD step. We also simulated spherical clusters of lutetium. In this case we generated the clusters from hcp crystalline structure by taking the first, second, and so on up to 19th neighbors, and we selected five cluster models with the number of atoms $n=33,51,81,117,147$. For these spherical clusters we also performed the quenching procedure. The three-dimensional structures of these clusters are presented in Fig. 3(b).

The binding energy, namely, the average interaction energy per atom in the cluster, versus the cluster size, i.e., the number of atoms in the cluster, is plotted for the most stable structures in Fig. 4. The average binding energy per atom decreases as the cluster size increases, and shows an exponential-like decay, as expected. The change is fast for the sizes $n=3-13$. However, the variation of binding energy with respect to the cluster size for the sizes $n=13-147$ is relatively slow. The general decay behavior in the average binding energy with respect to the cluster size is common for almost all microclusters. Since we scaled the PEF during parametrization to the bulk cohesive energy, as $n\rightarrow\infty$ this curve should go asymptoticly to the bulk cohesive energy value of -4.40 eV.

For isolated clusters the average binding energy per atom in the cluster $E_b=\Phi/N$ may be expressed as a function of cluster size N [3]:

$$E_b=E_v+E_sN^{-1/3}+E_cN^{-2/3}, \tag{4.1}$$

where the coefficients E_v, E_s, and E_c correspond to the volume, surface, and curvature energies of the particles forming the cluster, respectively. The corresponding plot for this expression, Eq. (4.1), is given in Fig. 5. The linear fit to this equation gives $E_v=-2.112$ and $E_s=2.509$, the quadratic fit gives $E_v=-2.055$, $E_s=2.194$, and $E_c=0.374$. The volume energy term should be equal to the bulk cohesive energy value of -4.40. The reason for the difference between the calculated value from the fit and the experimental value is that the clusters considered in the present study are not large enough. As the cluster size increases, the calculated volume energy approaches the bulk cohesive energy.

The most stable structures of the microclusters with sizes $n=3-7$ have a regular symmetry. The corresponding point groups of these clusters are shown in Fig. 3(a). On the other hand, the clusters for the sizes $n=8-12$, have no regular symmetry. Lu_{13} has the highest symmetry, I_h. The bond lengths shown on the pictures correspond to the average nearest-neighbor distance values at the last MD step. The spherical clusters almost kept their spherical form after the simulation, but atoms on the surface region reconstructed slightly with respect to the original positions. The estimated interatomic distances in the microclusters obey the general relation ($r_e<r<d_{nn}$), where r_e is the dimer distance, d_{nn} is the nearest-neighbor distance in the crystal, and r is the average nearest-neighbor distance in the cluster. Since we determine the effective pair potential parameters using crystal structure information, the estimated average interatomic distances in the clusters might be slightly larger than the actual values.

We have investigated the structural stability and energetics of isolated lutetium microclusters containing 3 to 147 atoms. As a conclusion we may say that lutetium microclusters prefer to form three-dimensional compact structures. Information about the isolated microclusters of lutetium does not exist in the literature, therefore we are not able to compare the present results with experimental and other theoretical works. We should say that the MD results obtained in this work are qualitative and we believe that they represent a correct trend. The electronic and geometric structure calculations by RDFT for lutetium microclusters for $n=3-13$ are in progress in our laboratory.

ACKNOWLEDGMENTS

The authors would like to thank JAERI for financial support. One of the authors (Ş.E.) would like to thank the members of JAERI for their hospitality during the course of this work at Tokai.

[1] *Microclusters*, edited by S. Sugano, Y. Nishina, and S. Ohnishi (Springer-Verlag, Berlin, 1987).
[2] *Clusters of Atoms and Molecules*, edited by H. Haberland (Springer-Verlag, Berlin, 1994).
[3] *The Chemical Physics of Atomic and Molecular Clusters*, edited by G. Scoles (North-Holland, Amsterdam, 1990).
[4] Ş. Erkoç, Phys. Rep. **278**, 79 (1997).
[5] *Handbook on the Physics and Chemistry of Rare Earths*, edited by K.A. Gschneidner, Jr. and L. Eyring (North-Holland, Amsterdam, 1994), Vols. 17–19.
[6] *Handbook on the Physics and Chemistry of Rare Earths*, edited by K.A. Gschneidner, Jr. and L. Eyring (North-Holland, Amsterdam, 1995), Vol. 22.
[7] *CRC Handbook of Chemistry and Physics*, 78th ed. (CRC, Boca Raton, FL, 1997).
[8] *Density Functional Theory*, Vol. 337 of *Advanced Studies Institute, Series B: Physics*, edited by E.K.U. Gross and R.M. Dreizler (Plenum, New York, 1995); R.G. Parr and W. Yang, *Density Functional Theories of Atoms and Molecules* (Oxford University Press, Oxford, 1989).
[9] P. Pyykö, Chem. Rev. **97**, 597 (1997), and references therein.
[10] K. Balasubramanian, *Relativistic Effects in Chemistry* (Wiley, New York, 1997).
[11] T. Baştuğ, D. Heinemann, W.-D. Sepp, D. Kolb, and B. Fricke, Chem. Phys. Lett. **211**, 119 (1993).
[12] B. Fricke, W.-D. Sepp, T. Baştuğ, S. Varga, K. Shulze, J. Anton, and V. Pershina, Adv. Quantum Chem. **29**, 109 (1997).
[13] S.H. Vosko, L. Wilk, and M. Nusair, Can. J. Phys. **58**, 1200 (1980).
[14] A.D. Becke, Phys. Rev. A **38**, 3098 (1988).
[15] E. Engel, S. Keller, and R.M. Dreizler, Phys. Rev. A **53**, 1367 (1996).
[16] J. Meyer, W.-D. Sepp, B. Fricke, and A. Rosén, Comput. Phys. Commun. **96**, 263 (1996).
[17] T. Baştuğ, W.-D. Sepp, D. Kolb, B. Fricke, G. Te Velde, and E.J. Baerends, J. Phys. B **28**, 2325 (1995).
[18] P.M. Boerrigter, G. Te Velde, and E.J. Baerends, Int. J. Quantum Chem. **33**, 87 (1988); G. Te Velde and E.J. Bearends, J. Comput. Phys. **99**, 84 (1992).
[19] Ş. Erkoç, Z. Phys. D **32**, 257 (1994).
[20] R.W.G. Wyckoff, *Crystal Structures*, 2nd ed. (Interscience, New York, 1960), Vol. 1.
[21] C. Kittel, *Introduction to Solid State Physics*, 4th ed. (Wiley, New York, 1971).
[22] H. Mehrez, S. Ciraci, C.Y. Fong, and Ş. Erkoç, J. Phys.: Condens. Matter **9**, 10 843 (1997).